# The Performance of Structured Packings in Trickle-Bed Reactors

Frank, M.J.W.; Kuipers, J.A.M.; Versteeg, G.F.; Swaaij, W.P.M. van

*Published in:*
Chemical Engineering Research and Design

*DOI:*
10.1205/026387699526566



*Publication date:*
1999

IChemE

0263–8762/99/$10.00+0.00

Trans IChemE, Vol 77, Part A, October 1999

# THE PERFORMANCE OF STRUCTURED PACKINGS IN TRICKLE-BED REACTORS

**M. J. W. FRANK, J. A. M. KUIPERS, G. F. VERSTEEG and W. P. M. VAN SWAAIJ**

*Department of Chemical Engineering, Twente University, Enschede, The Netherlands*

An experimental study was carried out to investigate whether the use of structured packings might improve the mass transfer characteristics and the catalyst effectiveness of a trickle-bed reactor. Therefore, the performances of a structured packing, consisting of KATAPAK elements, and a dumped packing, consisting of small diameter spherical particles, have been compared for both a chemisorption process and a process where a heterogeneously catalysed chemical reaction is carried out. The chemisorption of $CO_2$ in aqueous amine solutions and the hydrogenation of $\alpha$-methylstyrene catalysed by palladium on $\gamma$-alumina were chosen as model reactions, respectively. The performance of the trickle-bed reactor was quantified by measuring the specific gas-liquid contact area and the volumetric liquid-side mass transfer coefficient in the case of the chemisorption process and the conversion rate in the case of the heterogeneously catalysed chemical reaction. These parameters were measured for both packing types as a function of a number of process parameters. In this paper, the experimental results are presented and a comparison is made of the performances of the two packing types for both types of processes. Both packing types showed similar mass transfer characteristics as well as volumetric conversion rates. However, the structured packing showed a much higher contact efficiency as well as a much higher catalyst effectiveness. A significant improvement is therefore expected when a structured packing is used with a higher specific geometrical area than that applied in this study. Furthermore, the structured packing is favoured in the case of fast exothermic liquid-phase reactions.

*Keywords: trickle-bed reactor; structured packing; gas-liquid contact area; mass transfer; hydrogenation*

## INTRODUCTION

Trickle-bed reactors are packed columns where a liquid and a gas flow cocurrently downwards, while a chemical reaction takes place in the liquid phase. In many cases the chemical reaction is catalysed by the solid phase. The liquid forms a thin film on the packing whereas the gas is the continuous phase. The reactor can also be operated countercurrently or cocurrently upwards, but these flow types are less frequently encountered in industrial columns.

Trickle-bed reactors are widely applied and can be found in the petroleum industry, in the petrochemical industry, in waste water treatment units and in the biological, agro-food and pharmaceutical industries. Examples of applications are: hydrodesulphurization (Schuit and Gates, 1973[1]), hydrocracking of heavy or residual oil stocks, the hydrofinishing or hydrotreating of lubricating oils, demetallization, denitrification of gas-oils, isomerization of cyclopropane, hydrogenation of benzene and naphthenic lube oil distillate (Satterfield,1975[2]; Morsi *et al.*, 1984[3]), hydrogenation and oxidation of organic compounds (Morsi *et al.*,[3] Ramachandran *et al.*, 1987[4]) and oxidation of dilute aqueous solutions of organic pollutants.

The main advantages of the trickle-bed reactor compared with the slurry reactor, another often used three-phase reactor, are the plug flow type of flow pattern leading to higher reaction conversions, a high catalyst loading per unit volume of the liquid resulting in less occurrence of homogeneous side reactions and higher selectivity, the possibility of operating at higher pressure and temperature, a low pressure drop and a greater flexibility with respect to production rates and operating conditions used. The main disadvantages are the lower catalyst effectiveness due to the large catalyst particle size, bad heat removal due to poor radial mixing of heat, which becomes important in the case of highly exothermic reactions, and inferior mass transfer characteristics due to the fact that the majority of the industrially applied trickle-bed reactors are operated at low gas and liquid flow rates.

A possible solution to these problems may be the use of structured packings, since they are claimed to have the following advantages compared with dumped packings: higher gas and liquid loadings are possible, much lower pressure drops, better mass transfer characteristics (Meier *et al.*, 1977[5]) and higher catalyst effectiveness (DeGarmo, 1992[6]). The main disadvantage of the structured packing is its higher production cost compared to dumped packings, but due to an increasing number of manufacturers and increasing sales, the prices for such packings will still decrease.

For trickle-bed reactors, however, the use of structured packings is still unknown. Up to now the structured packings are mainly used as a means to create sufficient gas-liquid contact area. The main application of structured packings can be found in the petrochemical industry as it is estimated that nowadays 25% of all refinery vacuum towers worldwide are now fitted with structured packings (Laso *et al.*, 1995[7]). Oleochemicals such as glycerol, fatty acids, fatty alcohols and wax esters are refined by distillation and deodorization. As these products are extremely heat sensitive, it is necessary that they are distilled at low temperatures and therefore at vacuum pressure. Consequently, the pressure drop per stage must be very low. Furthermore, the residence time must be very short. These features are encountered by using a structured packing (Johannisbauer and Jeromin, 1992[8]).

Applications where the packing also serves as a catalyst are seldom reported in literature. DeGarmo[6] reports a reactive distillation process for the production of ethers using Katamax structured packing, developed by Koch Engineering Co.. The Katamax structured packing consists of ordered flow channels, in which intersections promote mixing and radial distribution of the rising vapour and the descending liquid phase. It holds the solid catalyst in screen envelopes, which allows the liquid phase to effectively reach the catalyst. Krafczyk and Gmehling, 1994[9] also successfully applied a structured packing for the reactive section in a catalytic distillation column producing methylacetate. Commercial acidic ion-exchange pellets, which is the actual catalyst, were fixed on a KATAPAK®-MK structured packing, developed by Sulzer.

Structured packings look very promising, but have not been applied in trickle-bed reactors so far. In this paper, therefore, a comparison will be made between the performance of a dumped packing (porous alumina spheres) and a structured packing (KATAPAK®-MK from Sulzer) in a trickle-bed reactor. Two types of applications will be investigated:

1. The only function of the packing is to create a sufficient amount of gas-liquid contact area: a gas is absorbed into a liquid mixture where a non-catalysed chemical reaction takes place between the absorbed species and a liquid component. The chemisorption of carbon dioxide in aqueous amine solutions was chosen as a model system. Important parameters in this case are the specific gas-liquid contact area and the volumetric liquid-side mass transfer coefficient.
2. The packing also serves as the catalyst and a fast heterogeneously catalysed chemical reaction is carried out. The hydrogenation of $\alpha$-methylstyrene, catalysed by palladium on $\gamma$-aluminium oxide, was chosen as a model reaction. The important parameter in this case is the conversion rate.

## $CO_2$—CHEMISORPTION

In this section, the performance of the structured packing as a means to create gas-liquid contact area will be investigated. It was chosen to study the chemisorption of $CO_2$ in aqueous amine solutions. By choosing different amines the chemical reaction rate can be varied. Depending on the rate of the chemical reaction in the liquid phase, the gas absorption rate depends on the specific gas-liquid contact area $a_{GL}$ (fast chemical reactions) or on the volumetric liquid-side mass transfer coefficient $k_L a_{GL}$ (slow chemical reactions). Large values of these quantities will lead to high production rates per unity reactor volume. Both parameters depend on the type of packing used in the column, as well as the flow rates and the properties of the fluids. Dumped packings have been examined in many previous studies[2,10–22], but for structured packings used in cocurrent down flow absorption columns very little has been published[23–27]. An extensive review is presented in Frank, 1996[27].

### Experimental Setup

*Apparatus*

Figure 1 shows a flow scheme of the experimental setup. The experiments have been carried out in a thermostatted trickle-bed column of glass with an internal diameter of 36 mm (in the case of dumped packings) or 38 mm (in the case of the structured packing) and a height of 0.50 m. The trickle-bed column was operated in cocurrent downflow. The column was provided with two taps to measure the pressure drop across the bed using a U-tube filled with water.

*Liquid stream*

Demineralized water containing DiEthanolAmine (from Janssen Chimica, 99% purity) or TriEthanolAmine (from Janssen Chimica, 98% purity, major impurity is water) was fed from a 150 litre storage vessel, where it was stripped with nitrogen, to the column where the liquid flow rate was controlled with a Brooks Rotameter. Before entering the reactor the liquid was heated to the reactor temperature. The liquid distributor, which was situated 1 cm above the packing in the column, consisted of a shaft with 4 holes at the bottom and 8 arms with each 1 hole (i.e. 12000 feed points/$m^2$). At the end of the column the liquid was collected in a gas-liquid separator. The amount of liquid present in the separator was kept constant with a level controller. The liquid flowing out of the separator was collected in a second vessel. If the second storage vessel was full, the liquid mixture was sent to the scrubber, where the $CO_2$ was stripped from the liquid phase by boiling it. The amine was retained completely and the liquid mixture could be used for subsequent experiments. The liquid phase showed no or very little degradation of the used amines. The analysis of the entering liquid mixture was carried out by acid titration with 1 M HCl (Mettler DL25 Titrator).

*Gas stream*

The gas flow rates of $N_2$ and $CO_2$ were controlled with two separate mass flow controllers (Brooks, type 5850 TR). The gas mixture was pre-saturated with water at reactor temperature and sent to a gas distribution section before entering the trickle-bed column. The gas leaving the gas-liquid separator was split: one part was sent to the analysing section whereas the other part was sent through a flow indicator to the vent. The gas phase was analysed using a TCD-gas chromatograph (Varian 3300).

The physical properties of the liquid mixtures and gases

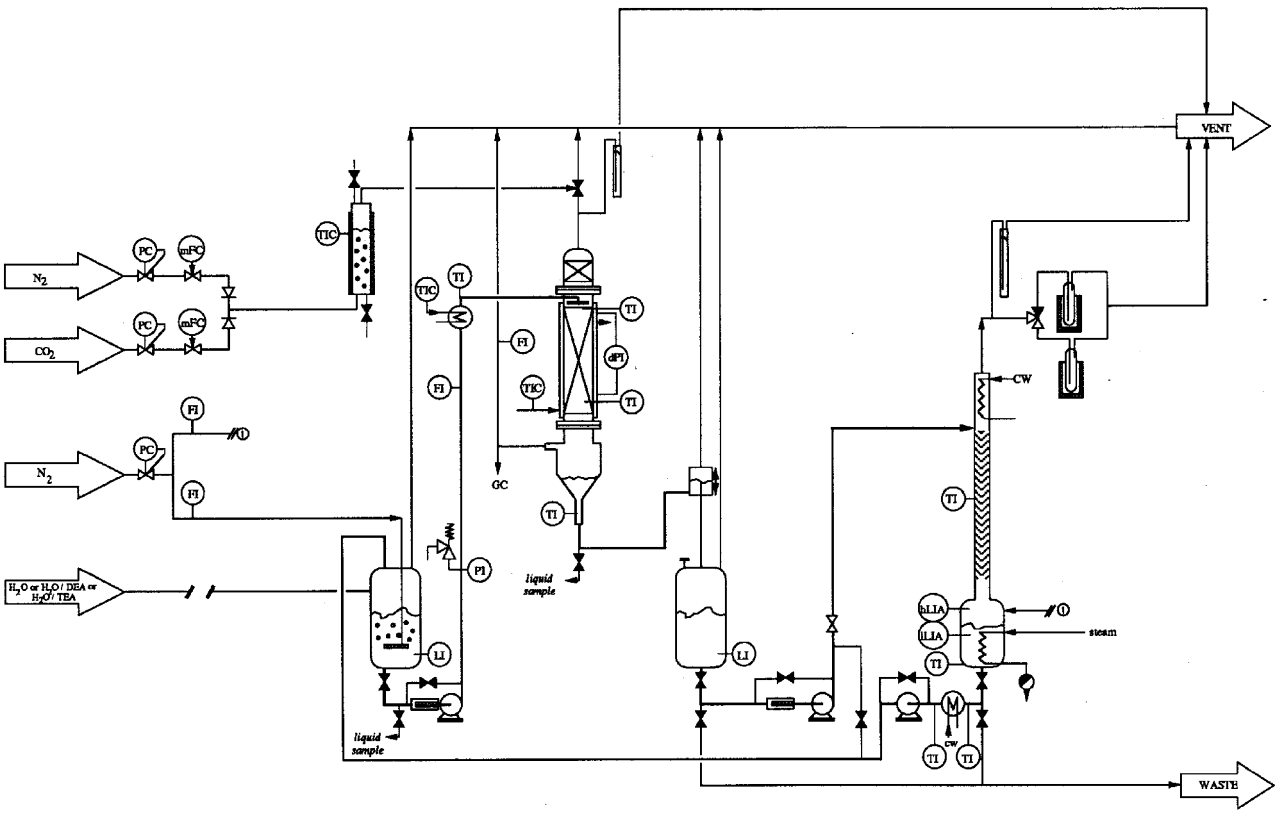


*Figure 1.* Flow scheme of the experimental setup for the chemisorption experiments.

which were used during the experiments are presented in Table 1.

*Packing*

Two types of packing were used: porous alumina spheres and KATAPAK®-MK structured packing elements. The spheres were derived from Engelhard and had an average diameter of 3.3. mm. The properties of the porous alumina spheres are given in Table 2. The structured packing elements were made by Sulzer Chemtech. They consist of a FeCr alloy support with an alumina layer of about 60 μm thick. Further details are given in Table 2 and a drawing of one element is shown in Figure 2. To prevent the liquid from flowing along the wall, as the elements are not perfectly cylindrical, the elements are covered tightly by a plastic overheadsheet (3M) before inserting them into the reactor.

## Experimental Procedures

*Specific gas-liquid contact area*

The specific gas-liquid contact area was determined by absorption of carbon dioxide from a nitrogen/carbon dioxide gas mixture into an aqueous di-ethanol-amine solution. $CO_2$ reacts fast with DEA in the liquid phase, resulting in enhancement of absorption compared with physical absorption, and consequently the absorption rate is governed by the amount of gas-liquid interface. The following expression was used to calculate $a_{GL}$ from measured in- and outlet carbon dioxide concentrations in the gas phase[27]:

$$\ln\left(\frac{C_{CO_2,G,in}}{C_{CO_2,G,out}}\right) = \frac{\sqrt{k_{app}D_{CO_2}}a_{GL}m}{U_G}H + \text{constant} \qquad (1)$$

$C_{CO_2,G,in}$ and $C_{CO_2,G,out}$ are the $CO_2$ concentrations in the in- and outlet gas stream of the reactor respectively, $k_{app}$ is the volumetric reaction rate constant of $CO_2$ with the amine, $D_{CO_2}$ is the diffusivity of $CO_2$ in the amine solution, $m$ is the solubility of $CO_2$ in the amine solution, $U_G$ is the superficial gas velocity and $H$ is the packing height.

The $CO_2$-concentrations in respectively the in- and outlet gas stream were measured at different packing heights. The interfacial area $a_{GL}$ can subsequently be calculated from

*Table 1.* Properties of the gases and liquids at $T = 313$ K.

| | $\rho$ [kg m$^{-3}$] | $\eta$ [mPa s] | $\sigma$ [N m$^{-1}$] |
|---|---|---|---|
| water | 992 | 0.65 | 0.068 |
| water/Tri-Ethanol-Amine $C_{TEAL} = 150$ mol m$^{-3}$ | 995 | 0.68 | 0.058 |
| water/Di-Ethanol-Amine $C_{DEAL} = 150$ mol m$^{-3}$ | 994 | 0.69 | - |
| nitrogen | 1.09 | 0.018 | - |
| carbon dioxide | 1.71 | 0.015 | - |

*Table 2.* Catalyst characteristics.

| Spheres from Engelhard | 1 | 2 | 3 |
|---|---|---|---|
| particle diameter, mm | 3.3 | | |
| material | $\gamma$-$Al_2O_3$ | | |
| BET-surface, $m^2g^{-1}$ | 87 | 82 | |
| thickness impregnated layer, mm | 0.30 | 0.25 | - |
| palladium content, wt% | 0.45 | 0.30 | 0 |
| solid density, $kg\,m^{-3}$ | 3400 | | |
| particle density, $kg\,m^{-3}$ | 1150 | | |
| particle porosity | 0.67 | | |
| bed porosity | 0.39 | | |
| geometrical contact area, $m^2m^{-3}$ bed | 1100 | | |
| **Structured packing KATAPAK®-MK from Sulzer impregnated with Pd by Engelhard** | **1** | **2** | **3** |
| diameter, mm | 38 | | |
| length, mm | 100 | | |
| corrugation amplitude, mm | 4 | | |
| channel angle to flow axis, ° | 45 | | |
| geometrical contact area, $m^2m^{-3}$ bed | 650 | | |
| porosity | 0.85 | | |
| material | FeCr-alloy | | |
| washcoat | $\gamma$-$Al_2O_3$ | | |
| thickness of washcoat, mm | 0.06 | | |
| BET-surface, $m^2g^{-1}$ | 63 | | |
| palladium content, wt% of washcoat | 4 | 4 | 0 |
| gauze collars | no | yes | no |

equation (1) by plotting the natural logarithm of the ratio of the $CO_2$-concentrations in the in- and outlet gas stream respectively, versus the packing height. The physical and chemical parameters which have been used to calculate $a_{GL}$ are listed in Table 3. The operating conditions are given in Table 4. Measurements were obtained by decreasing the liquid flow rate starting from operation at the maximum liquid flow rate.

*Volumetric liquid-side mass transfer coefficient*

The volumetric liquid-side mass transfer coefficients $k_La_{GL}$ were determined by absorption of carbon dioxide from a nitrogen/carbon dioxide gas mixture into an aqueous tri-ethanol-amine solution. $CO_2$ reacts slowly with TEA in the liquid phase, resulting in a small enhancement factor, and also a small concentration of $CO_2$ in the liquid bulk. Consequently, the absorption rate is governed by the volumetric mass transfer coefficient. The following expression is used to calculate $k_La_{GL}$ from measured in- and outlet carbon dioxide concentrations in the gas phase[27]:

$$\ln\left(\frac{C_{CO_2,G,in}}{C_{CO_2,G,out}}\right) = \frac{mk_La_{GL}}{U_G}\frac{Ha\,\tanh(Ha) + Ha^2(AL-1)}{1 + Ha\,\tanh(Ha)(AL-1)} \times H + \text{constant} \qquad (2)$$

*Table 3.* Physical and chemical parameters at $T = 313$ K used for determination of $a_{GL}$.

| | |
|---|---|
| $k_{app} \approx 31 + 0.36\,(C_{DEA,L} - 125)\ s^{-1}$ | Versteeg and Oyevaar[38]; Littel[39] |
| $D_{CO2} = 2.6\times 10^{-9}\ m^2s^{-1}$ | Versteeg[40] |
| $D_{DEA} = 1.1\times 10^{-9}\ m^2s^{-1}$ | Snijder[41] |
| $m = 0.628$ | Versteeg[40]; Littel[39] |
| $120 < C_{DEA,L,in} < 145\ mol\,m^{-3}$ | |
| $y_{CO_2,in} = 0.05$ | |

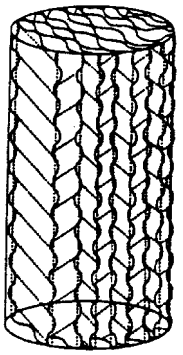

*Figure 2.* Drawing of a KATAPAK®-MK element.

*Ha* is a dimensionless number containing the reaction rate constant $k_{app}$ and the mass transfer coefficient $k_L$ and *AL* is the Hinterland ratio which is a function of the mass transfer coefficient $k_L$, the liquid holdup and the specific gas-liquid contact area $a_{GL}$.

The $CO_2$-concentrations in the in- and outlet gas stream respectively, were measured as a function of the packing height. By plotting the natural logarithm of the ratio of the $CO_2$-concentrations in the in- and outlet gas stream respectively versus the length of the bed, $k_La_{GL}$ can be calculated from the slope using equation (2). However, to calculate $k_La_{GL}$ from equation (2), knowledge of the specific gas-liquid contact area $a_{GL}$ is required. The experimental values of $a_{GL}$ were used. The physical and chemical parameters which were used for calculating $k_La_{GL}$ are listed in Table 5. The operating conditions are given in Table 4. Measurements were obtained by decreasing the liquid flow rate starting from operation at the maximum liquid flow rate.

## Experimental Results

*Specific gas-liquid contact area*

In Figures 3a and 3b, the experimentally determined specific gas-liquid contact area $a_{GL}$ is shown as a function of the liquid flow rate for the porous alumina spheres and the structured packing elements, respectively. The uncertainty in the $a_{GL}$ values is estimated as 20%, which is due to the

*Table 4.* Operating conditions chemisorption experiments.

| | |
|---|---|
| pressure, bar | 1 |
| temperature, K | 313 |
| liquid flow rate, $mm\,s^{-1}$ | $1 < U_L < 22$ |
| gas flow rate, $mm\,s^{-1}$ | $10 < U_G < 100$ |
| packing height, m | $0.10 < H < 0.50$ |

*Table 5.* Physical and chemical parameters at $T = 313$ K used for determination of $k_La_{GL}$.

| | |
|---|---|
| $k_{app} = 0.0076\ C_{TEA,L}\ s^{-1}$ | Littel[39] |
| $D_{CO2} = 2.6\times 10^{-9}\ m^2s^{-1}$ | Versteeg[40] |
| $m = 0.621$ | Versteeg[40]; Littel[39] |
| $C_{TEA,L,in} = 150$ | |
| $y_{CO_2,in} = 0.10$ | |

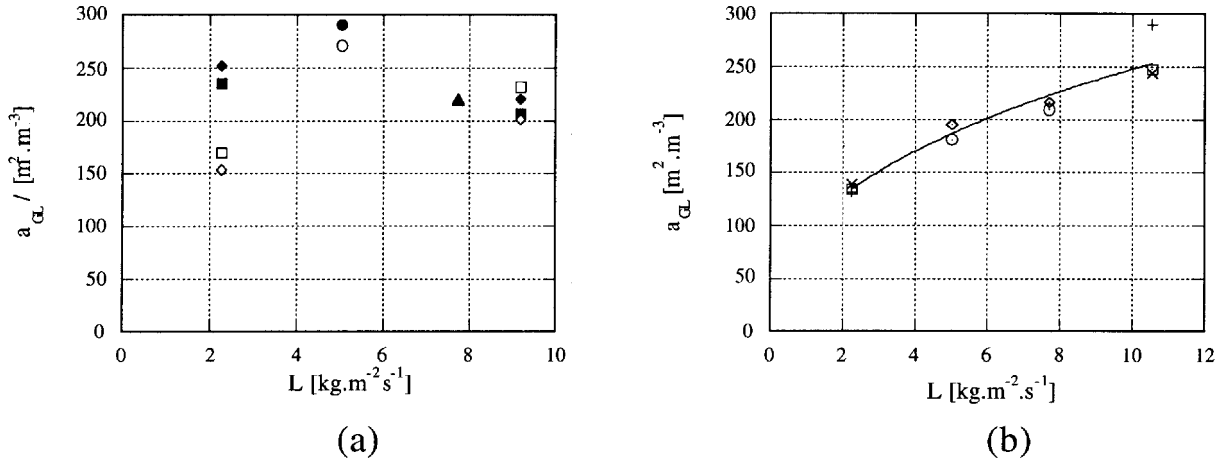


*Figure 3.* Measured interfacial areas as function of gas and liquid flow rate in case of (a) porous alumina spheres and (b) structured packing KATAPAK®-MK. (a) (o) $G = 0.011$ kg m$^{-2}$s$^{-1}$, (□) $G = 0.022$, (Δ) $G = 0.034$, (◇) $G = 0.045$, closed symbols: upper branch, open symbols: lower branch. (b): (o) $G = 0.011$ kg m$^{-2}$s$^{-1}$, (□) $G = 0.022$, (◇) $G = 0.034$, (x) $G = 0.045$, (+) $G = 0.090$, ( —— ) equation (3).

error made in determining the slope of equation (1) and the uncertainty in $k_{app}$.

From Figure 3a, it can be concluded that for the porous alumina spheres the gas load $G$ has no significant influence. The liquid load $L$ shows an optimum at $L = 5$ kg m$^{-2}$ s$^{-1}$. This finding is in accordance with what is known in the literature for conventional beds: beyond a certain point particle wetting is not a problem, but pockets of stagnant fluid will develop, which decrease the mass transfer rate. The average value of the specific gas-liquid contact areas found for the porous alumina spheres is $240 \pm 30$ m$^{-1}$.

For the structured packing specific interfacial areas are found which range between 130 and 300 m$^{-1}$. The contact area is independent of gas flow rate, but it increases with increasing liquid flow rate and can be correlated with:

$$a_{GL} = 95\, L^{0.4} \qquad (3)$$

The increase of $a_{GL}$ with $L$ is due to an increase of liquid holdup which leads to an increased coverage of the packing surface. The development of pockets of stagnant fluid is no problem here due to the high porosity of the packing.

*Comparison with literature*

The present experimental values for the specific gas-liquid contact areas for the porous alumina spheres are in the same order of magnitude as the values reported by Mahajani and Sharma[17]. They also coincide with the lowest values found by Lara-Marquez *et al.*[21] and are well described by the correlation from Fukushima and Kusaka[15]. The present data did not agree with $a_{GL}$ calculated from the correlations from Morsi and Charpentier[18], Midoux *et al.*[19] and Wild *et al.*[22]. These three correlations predict too low values with maximum deviations of 65, 75 and 90%, respectively.

Equation (3), valid for the structured packing, does agree with the expression reported by Shi and Mersmann[28] and possesses the same dependence of $a_{GL}$ with respect to the liquid loading $L$. The correlation of Henriques de Brito *et al.*[26] also predicts reasonably well the dependence of $a_{GL}$ on $L$ but predicts values which are too high by up to a factor of 4. The present results, however, do not agree with the findings of Weiland *et al.*[25] who reported $a_{GL}$ to be a strong function of the gas flow rate whereas it is independent of the liquid flow rate.

*Volumetric liquid-side mass transfer coefficient*

In Figures 4a and 4b, the experimentally determined volumetric liquid-side mass transfer coefficient $k_La_{GL}$ is shown as a function of the liquid flow rate for the porous alumina spheres and the structured packing elements, respectively. The uncertainty in the $k_La_{GL}$ values is estimated as 30%.

From an examination of the results obtained for the porous alumina spheres, it can be concluded that for $L > 4$ kg m$^{-2}$ s$^{-1}$, $k_La_{GL}$ is not a strong function of the liquid and gas loads and can roughly be taken as equal to 0.015 s$^{-1}$. However, for the smallest liquid load the mass transfer coefficient is significantly lower: $k_La_{GL} \approx 0.009$ s$^{-1}$.

A representative value for the liquid-side mass transfer coefficient can be obtained by taking the ratio of $k_La_{GL}$ and the average experimental value of $a_{GL}$ presented in the previous section. This gives: $k_L = 4 \times 10^{-5}$ m s$^{-1}$ at $L = 2$ kg m$^{-2}$ s$^{-1}$ and $k_L \approx 7 \times 10^{-5}$ m s$^{-1}$ for liquid loads ranging from 4 to 10 kg m$^{-2}$ s$^{-1}$.

For the structured packing, the volumetric liquid-side mass transfer coefficients are found to range between 0.005 and 0.025 s$^{-1}$. The volumetric mass transfer coefficient is not a clear function of gas flow rate, but it increases with increasing liquid flow rate, where the data can be correlated as follows:

$$k_La_{GL} = 0.0025\, L \qquad (4)$$

The increase of $k_La_{GL}$ with increasing liquid flow rate is only partially caused by the increase of $a_{GL}$ with $L$ according to equation (3), which indicates that $k_L$ varies with $L^{0.6}$. The calculated $k_L$ values range from $4 \times 10^{-5}$ m s$^{-1}$ at the lowest liquid flow rate up to $1 \times 10^{-4}$ m s$^{-1}$ at the highest liquid flow rate.

*Comparison with literature*

The experimental values of the volumetric liquid-side mass transfer coefficients for the porous alumina spheres coincide with the lowest values of the range given by Gianetto *et al.*[12]. They are a little bit lower than the

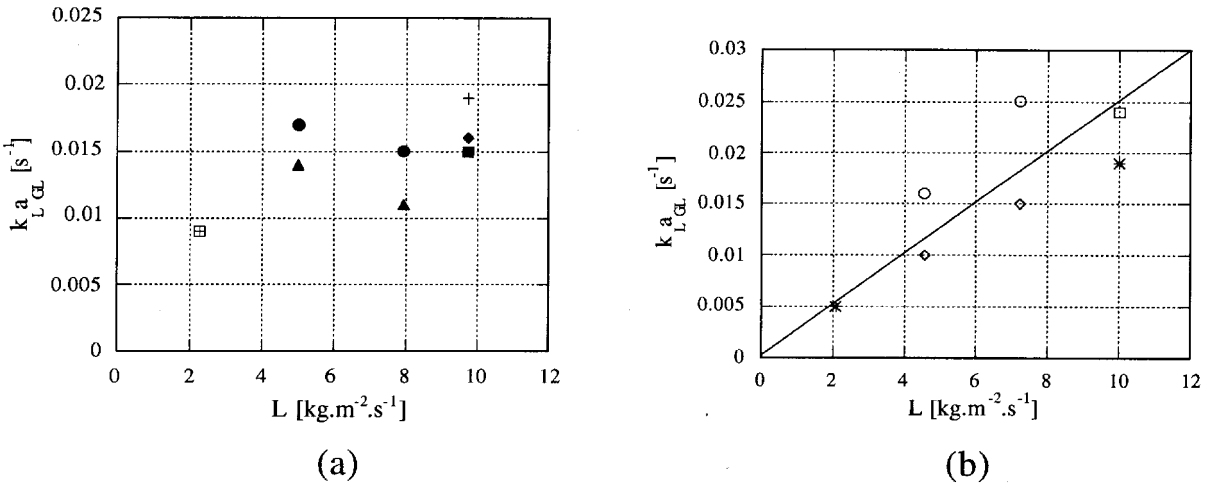


*Figure 4.* Measured volumetric liquid-side mass transfer coefficient as function of gas and liquid flow rate in case of (a) porous alumina spheres and (b) structured packing KATAPAK®-MK. (a) (o) $G = 0.011\ \mathrm{kg\,m^{-2}s^{-1}}$, (□) $G = 0.022\ \mathrm{kg\,m^{-2}s^{-1}}$, (Δ) $G = 0.034\ \mathrm{kg\,m^{-2}s^{-1}}$, (◇) $G = 0.045\ \mathrm{kg\,m^{-2}s^{-1}}$, closed symbols: upper branch, open symbols: lower branch, (+) $G = 0.090\ \mathrm{kg\,m^{-2}s^{-1}}$ upper branch (b): (o) $G = 0.011\ \mathrm{kg\,m^{-2}s^{-1}}$, (□) $G = 0.022\ \mathrm{kg\,m^{-2}s^{-1}}$, (◇) $G = 0.034\ \mathrm{kg\,m^{-2}s^{-1}}$, (x) $G = 0.045\ \mathrm{kg\,m^{-2}s^{-1}}$, (+) $G = 0.090\ \mathrm{kg\,m^{-2}s^{-1}}$, ( —— ) equation (4).

experimental values obtained by Mahajani and Sharma[17] and are well described by the correlations of Goto *et al.*[13] and Midoux *et al.*[19]. The correlation of Fukushima and Kusaka[15,16] predicts values which are 4 to 5 times too high. The correlation from Morsi[20] predicts, in general, too low values (up to a factor of 3). The equation of Wild[22], which is based on a vast amount of literature data, predicts $k_La_{GL}$-values which are 20 to 100 times too low!

The authors $k_L$ results obtained for the structured packing agree with the theoretical correlation given by Bravo *et al.*[23] which is based on the penetration theory for mass transfer. Their correlation predicts a dependence of $k_L$ with $L^{0.5}$. The results of Henriques de Brito *et al.*[24] indicate a dependence on $L$ with the power 0.3, which is too low. Their values for $k_L$ however, agree very well with the experimental results obtained in the present study. Furthermore, the authors' experimental values for the volumetric liquid-side mass transfer coefficient are in the same order of magnitude as those reported by Weiland *et al.*[25]

## Discussion

Despite a two-fold difference in geometrical areas of the porous alumina spheres and the structured packing respectively, the mass transfer characteristics for both packings are of the same order of magnitude, but show a different behaviour with respect to the liquid flow rate. The dumped packing showed values for $a_{GL}$ between 210 and $270\ \mathrm{m^2\,m^{-3}}$, independent of the gas flow rate, but with an optimum at $L = 5\ \mathrm{kg\,m^{-2}\,s^{-1}}$. The structured packing gave specific gas-liquid contact areas ranging from 150 to $300\ \mathrm{m^2\,m^{-3}}$ independent of the gas flow rate and increasing with increasing liquid flow rate: $a_{GL}$ = constant × $L^{0.4}$. Similar behaviour was found for the volumetric liquid-side mass transfer coefficient. The dumped packing showed an average value for $k_La_{GL}$ of about $0.015\ \mathrm{s^{-1}}$, independent of the liquid and gas flow rate. The structured packing gave values ranging between 0.005 and $0.025\ \mathrm{s^{-1}}$ independent of gas flow rate but increasing with increasing liquid flow rate: $k_La_{GL}$ = constant × $L$.

The experimentally found values for the specific gas-liquid contact area and the volumetric liquid-side mass transfer coefficient agree with some of the reported data in the literature. Large differences have, however, also been observed.

Based on Figures 3 and 4, it cannot be concluded that the mass transfer rates are improved due to the use of structured packings. However, if the contact efficiency is taken into account, defined as the ratio of the amount of gas-liquid interface area and the geometrical area of the packing, then the investigated structured packing (ranging from 0.2 to 0.5) shows a much higher value than the spherical packing (ranging from 0.15 to 0.25). Since structured packing elements are available in a wide variety of geometrical properties with geometrical area up to $1700\ \mathrm{m^2\,m^{-3}}$, still keeping the void fraction as high as 85%, this type of packing looks very promising in creating higher gas-liquid interface areas. They do not have the disadvantages of development of pockets with stagnant fluid and high pressure drop gradients, which would certainly occur when the geometrical area is increased in the case of the conventional packing type by applying smaller particles. Furthermore, since in the bed with the structured packing the liquid flow distribution is gradually improving with increasing liquid flow rate, improved mass transfer characteristics may be further expected at higher flow rates.

## HYDROGENATION OF α-METHYLSTYRENE

In this section, the performance of a structured packing as a catalyst support will be investigated by studying its behaviour under chemical reactive conditions and comparing this behaviour with that of a conventional catalyst packing. Conversion rates were measured in a trickle-bed reactor using a Pd-impregnated structured packing (KATAPAK®-MK from Sulzer) and Pd-containing porous alumina spheres. The hydrogenation of α-methylstyrene, catalysed by palladium on γ-aluminium oxide, was chosen as the model reaction. This chemical reaction is often used as a model reaction in studies involving trickle-bed reactors. An extensive review is given in Frank[27].

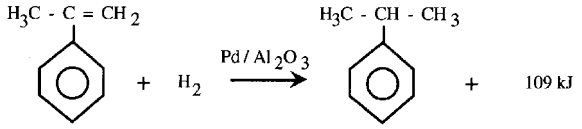


The exothermic reaction is irreversible and produces only cumene as a product, i.e. there are no side reactions. Furthermore, the homogeneous reaction does not take place, while the heterogeneous reaction proceeds with an appreciable rate at moderate temperatures and pressures. In addition, the reaction is quite representative of a wide class of volatile-reactant-limited, metal-catalysed, liquid-phase oxidations and hydrogenations.

The reaction may be assumed to be first order with respect to hydrogen and zero order with respect to AMS, provided that the mole fraction of AMS is larger than 0.10. Higher orders have, however, also been found. The experimentally determined values for the first order reaction rate constant show a large variation, which is partially caused by differences in internal diffusion limitation but probably also by differences in the preparation method of the catalyst, presence of liquid-phase impurities and in precautions taken during the experiments. The activation energy of the intrinsic reaction rate is 40 kJ mole$^{-1}$. Internal diffusion limitation lowers this value to 29 kJ mole$^{-1}$. Lower values of the activation energy will be caused by external mass transfer limitation.

Trickle-bed reactor studies using the hydrogenation of α-methylstyrene as a model reaction, using spherical catalyst particles, have shown that external mass transfer coefficients may increase due to the occurrence of a chemical reaction and that at low liquid flow rates partial wetting will prevail, causing a decrease of the local external mass transfer resistances. In addition, it was found that the conversion rate may become dependent on the fraction AMS due to diffusion limitation of AMS.

## Experimental Setup

*Apparatus*

Hydrogenation experiments were carried out in the same thermostatted double-walled glass column as was used for the $CO_2$ absorption experiments. The reactor is operated in cocurrent downflow. However, now the liquid is recycled and is therefore being used batch-wise, whereas the gas flows once through the column. The flow scheme of the experimental setup is shown in Figure 5.

*Liquid stream*

The liquid holdup in the recycle was about 0.4 to 0.5 kg. The liquid is fed to the top of the column using a distributor positioned 1 cm above the packing. For the lowest liquid flow rates the distributor didn't work well and the liquid formed one jet. The liquid flow rate is controlled using rotameters.

*Gas stream*

The gas is led through a prepacking for heating the gas before it is fed to the top of the column. The inlet gas flow rate is controlled by using Brooks mass flow controllers. At the outlet the gas flow rate is measured using a wet gas flow meter.

*Catalyst packing*

Two types of packing were used: palladium containing porous alumina spheres and KATAPAK®-MK structured packing elements (see Table 2). The spheres were derived from Engelhard and had an average diameter of 3.3 mm.

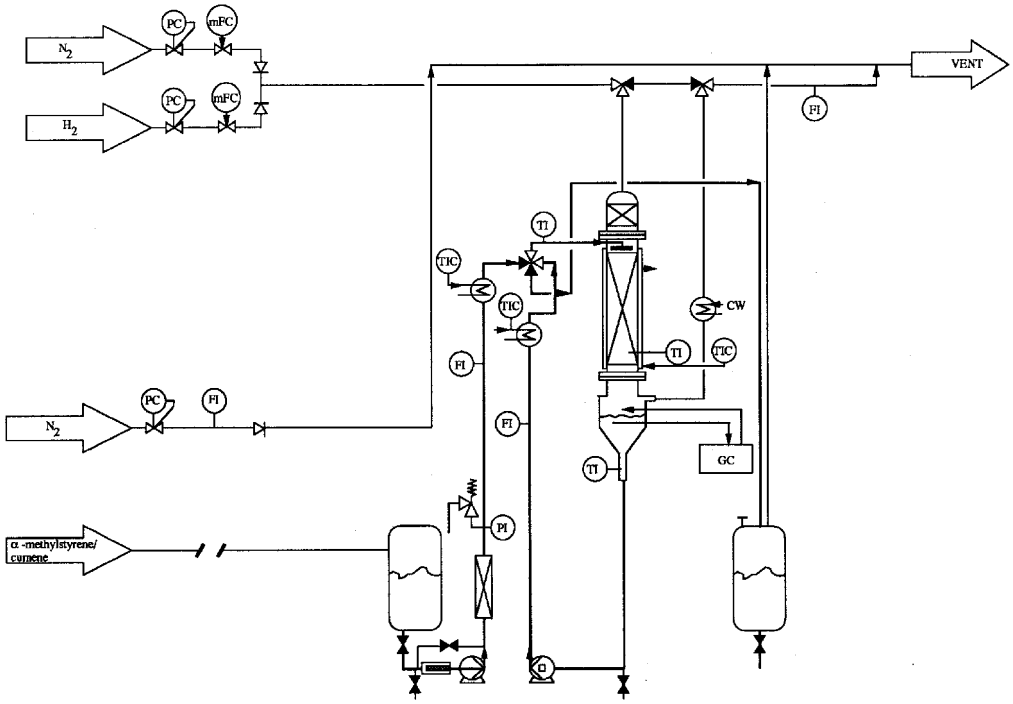


*Figure 5.* Flow scheme of the experimental setup for the hydrogenation experiments.

The palladium was deposited in the outer shell of the spheres. Catalyst particles with two different Pd concentrations were used: 0.3 and 0.45 wt% Pd. Scanning Auger Electron Spectroscopy revealed that the palladium was uniformly distributed in the outer layer and that the local concentrations were the same for the 0.3 and 0.45 wt% particles. Inert particles have also been used and were of the same type as the spheres which were used as a support for the catalytically active spheres. The structured packing elements were derived from Sulzer and consisted of several corrugated plates forming cylindrical elements (see Figure 2). The plates were coated with a thin layer of $\gamma$-alumina (0.060 mm). Impregnation of the alumina layer with palladium was done by Engelhard. Scanning Auger Electron Spectroscopy revealed that the palladium concentration in the alumina layer was the same as the local concentration in the spheres, except for the outer 0.015 mm where the Pd-concentration was approximately 8 times higher. The local palladium concentrations were estimated to amount 1.5 and 12 wt%, respectively. The average Pd-concentration is therefore approximately 4 wt%. As only one composition analysis has been made of a very small section of one packing element, it is very questionable whether the results are representative for the whole element and other elements. The elements were not perfectly cylindrical and voids will appear when positioned in the column. Bypassing of the liquid is likely to occur and radial distribution of the liquid will not be ideal if no precautions are taken. To circumvent these possible problems, the elements were wrapped tightly into a plastic sheet (3M overhead sheets) before inserting them into the column. Another precaution to avoid severe maldistribution of the liquid was tested: gauze collars at the top and the bottom of each element. These collars contact the reactor wall, leading the liquid flow on the wall into the packing element, resulting in a higher wetting efficiency.

*Chemicals*

Preliminary hydrogenation experiments in a stirred vessel showed that $\alpha$-methylstyrene derived from several companies and even chemicals from the same company, produced from a different batch, resulted in a variety of reaction rates. Therefore, all experiments were carried out with AMS from the same company and with the same lot number. AMS and cumene with a purity of 99% were derived from Merck. Hydrogenation experiments in a stirred vessel also showed that for some liquids the reaction rate could be increased by pretreating the liquid reactant with alumina powder. In this experimental setup this pretreatment was achieved by leading the liquid through a packed bed of alumina pellets before it is fed to the reactor. Hydrogen and nitrogen with a purity of 99.999% were derived from Hoekloos.

*Analysis*

The conversion rates were measured using two different methods. In the first method the change in hydrogen flow rate was measured whereas in the second method the liquid-phase composition was monitored by gas chromatography. Liquid from the gas-liquid separator was pumped through a small recycle, including the GC-injector valve. The conversion rates determined on basis of these two methods agreed within 5%. As well as the hydrogen consumption and the liquid-phase composition, the temperatures of the inlet liquid flow and the liquid flowing in the bottom of the bed are measured.

## Experimental Procedure

Prior to a series of experiments the reactor was filled with dry catalyst. Preliminary experiments in the trickle-bed reactor showed that if the particles contained liquid reactant at the start of an experiment, severe deactivation of the catalyst occurred. After filling the reactor with catalyst, it was heated to 65°C while nitrogen was fed to the reactor. After reaching the temperature of 65°C, hydrogen was passed through the reactor for 1 hour to activate the catalyst. Subsequently, nitrogen was fed to the reactor and when the temperature was lowered to 40°C, liquid is pumped from a 5 l storage vessel through the 4-way valve to the recycle. If the liquid level in the recycle reached a certain height in the gas-liquid separator, the 4-way valve was switched and the liquid was pumped at a high flow rate, together with a high gas flow rate through the reactor for 20 minutes. Impurities in the bed and tubes will be absorbed by the liquid and furthermore, the porous packing will be wetted. After draining the first liquid batch the recycle is filled again. The packing is fully wetted again by pumping the liquid through the recycle at a high flow rate for five minutes before setting the liquid flow rate to the desired value. Then the nitrogen flow is stopped and the reaction is started by setting the hydrogen flow rate to the desired value. During the experiment, which may last up to 7 hours, the outlet gas flow rate, the liquid-phase composition, the liquid inlet temperature and the bedtemperature were measured. At the end of each experiment the total liquid holdup was determined by weighing the wetted packing and the liquid drained from the recycle.

In the present study, the influences of the following parameters on the conversion rate were investigated: type of catalyst, liquid flow rate, gas flow rate, height of catalyst packing, reactor temperature, initial AMS-concentration and initial hydrogen fraction. A standard operating condition was chosen to provide a reference basis and the parameters were changed relative to this situation (see Table 6). If possible, the standard operating condition was created at the beginning of each experiment to check the activity of the catalyst packing. Independent pressure drop measurements showed that the transition from trickle flow regime to pulse flow regime for the spherical catalyst particles occurs at a liquid flow rate somewhere between 7 and 14 ml $s^{-1}$. As the liquid flow rate ranged from 1.5 to 25 ml $s^{-1}$, measurements were carried out in both flow

*Table 6.* Operating conditions hydrogenation experiments.

| Parameter | Standard run | Total range |
|---|---|---|
| catalyst type | 1 | 1,2, and 3 |
| liquid flow rate, ml $s^{-1}$ | 6.5 | 1.5–25 |
| gas flow rate, ml $s^{-1}$ | 40 | 10–80 |
| bed height, cm | 23 or 20 | 10–40 |
| reactor temperature, K | 313 | 293–333 |
| initial AMS-fraction | 1 | 0.2–1 |
| initial hydrogen fraction | 1 | 0.33–1 |
| fraction active spheres | 1 | 0.1–1 |
| pressure | atmospheric | – |

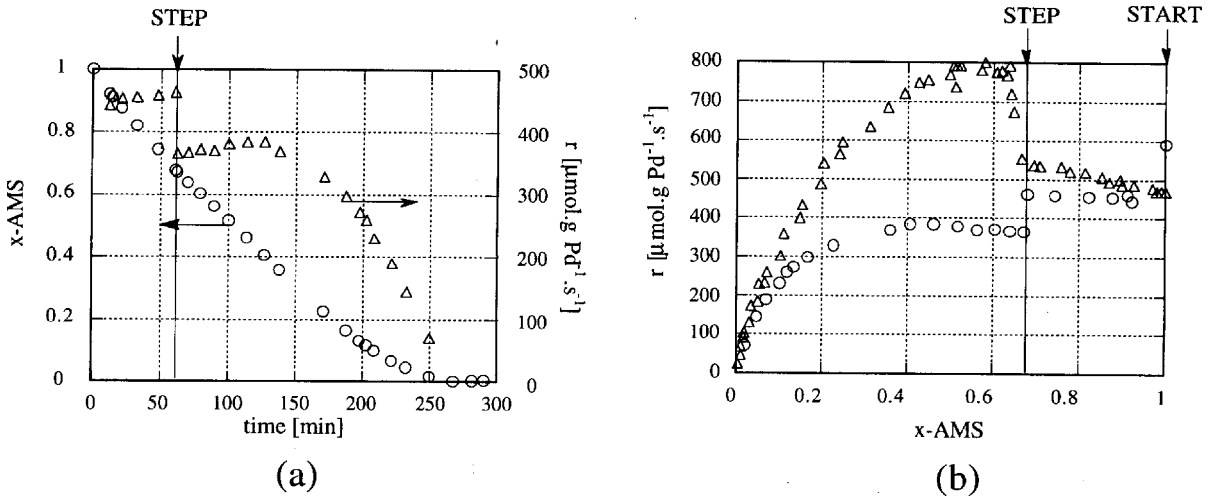


*Figure 6.* (a) Typical results for the conversion rate $r$ and fraction AMS as a function of process time for an experiment with catalyst spheres. Standard operating conditions at $t = 0$ min. At $t = 60$ min $\phi_L$ is changed from 6.5 to 10.6 ml s$^{-1}$. (b) The conversion rate as a function of liquid-phase composition. Standard operating conditions at $t = 0$ min. Liquid flow rate is changed from 6.5 ml s$^{-1}$ to respectively 10.6 ml s$^{-1}$ (o) and 2.7 ml s$^{-1}$ (Δ).

regimes. For the structured packings elements no such flow transition has been observed, within the limits of the operating conditions.

## Experimental Results

*Typical results of a trickle-bed experiment*

Figure 6a shows the typical results of a batch-wise hydrogenation experiment performed in the trickle-bed column using catalyst spheres. The consumption of hydrogen was measured as a function of time, from which data both the conversion rate and the fraction AMS have been calculated as a function of time. The liquid-phase composition calculated on the basis of hydrogen consumption agreed within several percents with the results of the liquid-phase composition measurements using the gas chromatograph. The experiment was started with standard operating conditions and pure AMS and after 60 min, the liquid flow rate was suddenly increased from 6.5 ml s$^{-1}$ to 10.6 ml s$^{-1}$ while the other parameters remained constant. It was shown with GC-analysis that only cumene was produced during the reaction and that complete conversion of AMS could be reached. It can be seen from Figure 6a that the observed conversion rate is approximately constant during the first 60 minutes. An increase of liquid flow rate results in an immediate decrease of conversion rate to another constant value. However, after a certain time ($t \approx$ 130 min) the conversion rate starts to decrease and gradually reaches zero for very high conversions. This phenomenon was reproducible and was also observed during other experiments. It seems that the conversion rate and the liquid-phase composition are related to each other. Therefore, the experimental conversion rates are plotted as a function of the fraction AMS, as shown in Figure 6b. The circles in this figure represent the results of the experiment shown in Figure 6a. In addition, results are shown (triangles) for an experiment where, after a certain time, the liquid flow rate was suddenly decreased from 6.5 ml s$^{-1}$ to 2.7 ml s$^{-1}$. This change resulted in an immediate increase of the conversion rate to a higher constant value. However, after a certain time the conversion rate again started to decrease gradually to zero. For all measurements with the spherical catalyst particles the experimental conversion rate curves could be divided into a liquid-phase composition-dependent part and a liquid-phase composition-independent part. The shape of the curves is in close agreement with results reported by Babcock *et al.*[29] for low hydrogen pressures ($P_{H_2} < 3$ atm) using a countercurrent trickle-bed reactor.

The experiments shown in Figure 6b show a reproducibility of the initial conversion rate (measured at standard operating conditions) within 10% where this rate roughly equals 500 µmole g Pd$^{-1}$ s$^{-1}$. Catalyst spheres which were used for six experimental runs in series (i.e. without refilling the column), showed no appreciable deactivation since all initial conversion rates ranged between 460 and 510 µmole g Pd$^{-1}$ s$^{-1}$. Experiments with other batches of catalyst, refilling of the column and AMS from different storage vessels showed that the maximum deviation from the typical initial conversion rate was approximately 20%.

The conclusion that the conversion rate can indeed be related to the liquid-phase composition, and does not change due to, e.g. deactivation, is confirmed by the results of the experiments with different initial AMS-fractions. Data from these runs lay on one curve when the conversion rate is plotted as a function of liquid-phase composition.

Experiments with catalyst spheres containing 0.30 wt% Pd (no. 2, see Table 2) showed approximately the same activity per gram palladium as catalyst spheres containing 0.45 wt% Pd (no.1). The inactive spheres (no. 3) showed no detectable hydrogenation activity, indicating that the reaction only proceeds in the presence of palladium.

A typical result for the batch-wise hydrogenation in a trickle-bed reactor using the KATAPAK® structured packing elements is shown in Figure 7 for standard operating conditions. The conversion rate has been expressed in mole m$^{-3}$ s$^{-1}$ instead of mole g Pd$^{-1}$ s$^{-1}$ as the amount of palladium per m$^3$ reactor is not known very accurately. The structured packing exhibits, compared to the results for the spheres presented in Figure 6b, a quite different behaviour with respect to the conversion rate as a function of the fraction AMS. The conversion rate at the

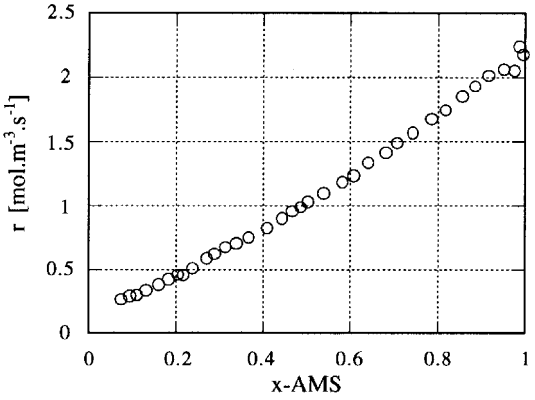


*Figure 7.* Typical result of a hydrogenation experiment with KATAPAK® structured packing. Conversion rate as function of liquid-phase composition for standard operating conditions.

start of a typical experiment approximately equals 2 mole $m^{-3}$ $s^{-1}$ and immediately starts to decrease. The $r$ versus $x$-AMS curve seems to intersect the $y$-axis at a positive value, however other experiments, where complete conversions were achieved, revealed that the conversion rate sharply decreases to zero for very low $x$-AMS values. The conversion rate at $x$-AMS = 1 is of the same order of magnitude as the volumetric conversion rate measured with the spheres at standard conditions: $r = 500$ μmole g $Pd^{-1}$ $s^{-1}$ corresponds to $r = 1.6$ mole $m^{-3}$ $s^{-1}$. If it is assumed that the entire geometrical surface area of the structured packing elements is used for chemical reaction, a volumetric conversion rate of 2 mole $m^{-3}$ $s^{-1}$ is equivalent to 1100 μmole g $Pd^{-1}$ $s^{-1}$, which indicates that the catalyst effectiveness for the structured packing is higher than the one for the conventional dumped packing.

The reproducibility of the results is quite (within 10%), independent of packing type. The same $r$ versus $x$-AMS curves were obtained in the case where the packing elements were wrapped in a sheet (type no. 1), where packing elements with a gauze collar were used (type no. 2) and even in the case where the packing elements without sheet and gauze collars were applied (type no. 1). If the packing elements did not fit well to the column wall, it could be observed visually that severe wall flow occurred and consequently lower conversion rates were measured. Packing elements no. 3 (see Table 2), which were not impregnated with palladium, showed, within the accuracy of the measuring method, no activity, indicating that the reaction only proceeds in the presence of palladium.

To check whether the decreasing conversion rate is indeed primarily related to the liquid-phase composition and not to process time, experiments have also been carried out for the structured packings using different initial AMS-fractions. A lower initial fraction of AMS resulted in a lower initial conversion rate, which is comparable to the measured conversion rate for this fraction in an experiment which was started with a higher initial fraction. It can be concluded, therefore, that the conversion rate is indeed related to the liquid-phase composition and not primarily to process time.

*Gas phase composition*

Figure 8a shows the effect of the hydrogen fraction in the inlet gas stream on the liquid-phase composition

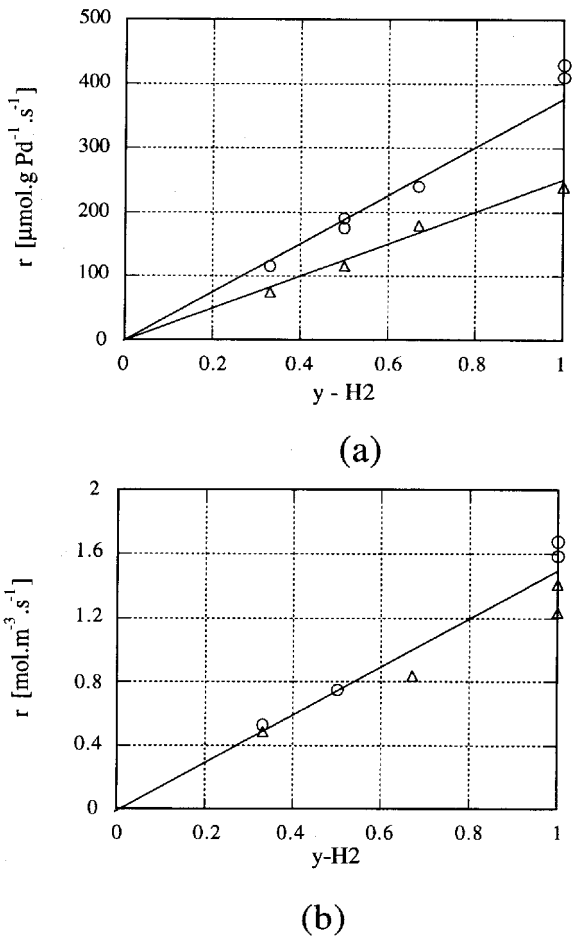


*Figure 8.* Conversion rate as function of the hydrogen fraction in inlet gas stream for (a) the catalyst spheres: $\phi_L = 6.5$ ml $s^{-1}$ (o) and $\phi_L = 21$ ml $s^{-1}$ (Δ) and (b) the structured packing at standard operating conditions: data from separate experimental runs using elements no. 2 are shown.

independent part of the conversion rate curve (see Figure 7) for the catalyst spheres. Data are shown for two liquid flow rates: 6.5 and 21.9 ml $s^{-1}$. Due to hydrogen consumption the actual average hydrogen fraction in the gas phase will be lower (i.e. 0.02 to 0.03) than the inlet value if a diluted gas phase (i,e, $y$-$H_2 < 1$) is fed to the reactor. From Figure 8a it follows that the liquid-phase composition independent conversion rate is approximately first order in hydrogen. The first order dependence with respect to hydrogen was also found in the situation where the conversion rate became dependent on the liquid-phase composition. The first order dependence is not in agreement with the results of Babcock *et al.*[29] and Cini and Harold[30], who reported an order of approximately 0.5 with respect to hydrogen.

Figure 8b shows the conversion rate, extrapolated to $x$-AMS = 1, as a function of the hydrogen fraction in the inlet gas stream for the structured packing at standard operating conditions. This figure shows that the hydrogenation process for the structured packing is also approximately first order with respect to hydrogen.

*Reactor temperature*

The influence of reactor temperature in the case of the spheres is shown in Figure 9a for $\phi_L = 6.5$ and 21 ml $s^{-1}$,

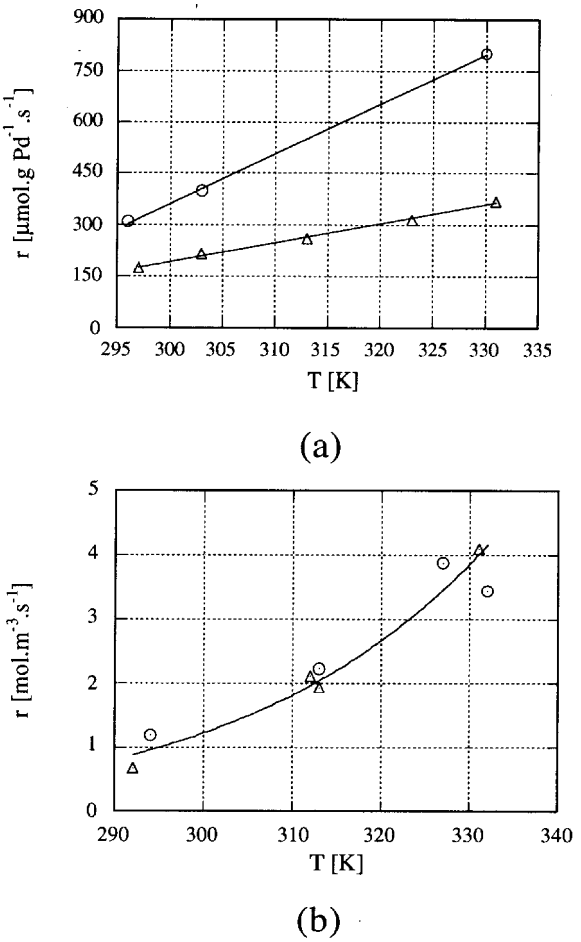


*Figure 9.* Influence of reactor temperature on conversion rate for (a) the catalyst spheres: standard operating conditions (o) and $\phi_L = 21$ ml s$^{-1}$ (Δ) and (b) the structured packing for for $\phi_L = 21.9$ ml s$^{-1}$ (o) and $\phi_L = 6.5$ ml s$^{-1}$ (Δ).

where the liquid-phase composition independent part of the conversion rate curve has been plotted as a function of the reactor inlet temperature. The corresponding energies of activation are 22 and 17 kJ mole$^{-1}$ for $\phi_L = 6.5$ and 21 ml s$^{-1}$, respectively. These values are comparable with the values found by Babcock *et al.*[29]

For the structured packing elements, the extrapolated conversion rates to $x$-AMS = 1 have been plotted as a function of temperature in Figure 9b ($\phi_L$ = 6.5 ml s$^{-1}$ and $\phi_L$ = 21.9 ml s$^{-1}$). The activation energies obtained equal 37 and 25 kJ mole$^{-1}$ for $\phi_L$ = 6.5 ml s$^{-1}$ and $\phi_L$ = 21.9 ml s$^{-1}$, respectively. These values are evidently higher compared to the corresponding values obtained for the catalytic spheres.

*Heat effects*

During the hydrogenation experiments, temperature rises in the liquid were observed. The temperature rise in the reactor for the catalyst spheres was typically 3 K for the standard situation. During the first minute of the experiment, however, the temperature rise was much higher (about 10 K). This phenomenon has also been reported by McManus *et al.*, 1993[31]. The temperature rise turned out to be a strong function of the actual conversion rate, the liquid flow rate and packing height, ranging from about 30 K at the lowest liquid flow rate to 1 K at the highest liquid flow rate. In one of the present experiments ($\phi_L = 2.7$ ml s$^{-1}$) hot spots were observed: exceptionally high temperature rises of respectively 40 and 80 K existed in the catalyst bed for two periods of 10 minutes.

Contrary to the experiments with the catalyst spheres, where the temperature could be measured in the centre of column, this was not possible for the structured packing, because only the temperature of the liquid flowing in the outer column section could be measured. The measured temperature rise during the experiment with standard operating conditions decreased gradually from 6 K at the start of an experiment to approximately 1 K when the reaction was almost completed. The maximum observed temperature rise was approximately 15 K in the case where the highest packing height was applied. No hot spots were observed during the experiments.

For all experiments, temperature rises have been compared with temperature rises which would prevail in the case where adiabatic operation of the reactor can be assumed[27]. From this it could be concluded that for both packing types the reactor may be considered as an adiabatic reactor, i.e. all heat which is produced due to chemical conversion is used to heat the liquid flowing through the catalyst bed.

Due to the adiabatic character of the reactor, axial temperature profiles will develop. Since the measured conversion rate will be influenced by this axial temperature profile, it seems logical to separate the thermal effects from other (i.e. hydrodynamic) effects. Frank[27] showed how the apparent conversion rate can be recalculated to the conversion rate related to the reactor inlet temperature:

$$r_{To} = A\left(1 - \exp\left(-\frac{r_{app}}{A}\right)\right) \tag{5}$$

where

$$A = \frac{C_L \phi_L C_P R T_0^2}{\Delta H_R V_R E_{app}} \tag{6}$$

To show the influence of the heat effects, the data presented in Figures 6b and 7 have been corrected for thermal effects. Comparison of the original data from Figure 6b and the corrected data, which are both shown in Figure 10a, reveals that for the spheres corrections for the axial temperature profile are very small for the highest liquid flow rate, whereas for the lowest liquid flow rate the corrected value is about 20% lower than the uncorrected value. Furthermore, it can be concluded that despite the temperature correction, there are still changes in conversion rate with changing liquid flow rate. Comparison of the original data from Figure 7 and the corrected data, both shown in Figure 10b, reveals that for the structured packing at medium liquid flow rate, temperature correction causes minor changes. Due to correction the conversion rate becomes more linear with liquid-phase composition in this case.

*Gas flow rate and packing height*

The catalyst spheres and the structured packing elements show the same trends for the conversion rates as a function of the gas flow rate and the packing height, respectively:

- for all experiments the influence of the gas flow rate on the measured conversion rate was found to be negligible.
- for all experiments an increase of measured conversion rate was found with increasing bed height. This effect is a

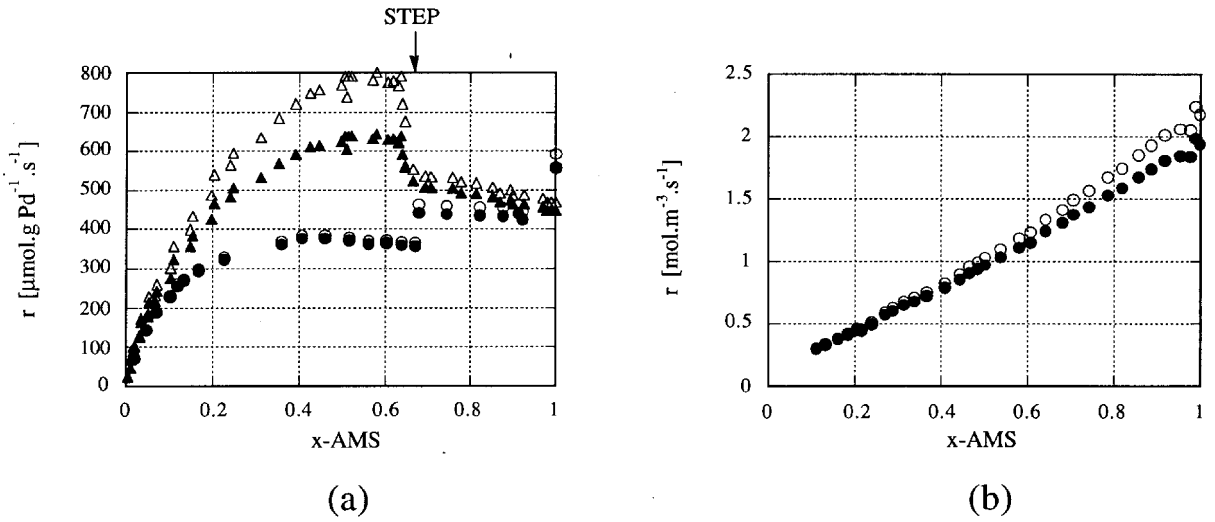


*Figure 10.* Conversion rates as a function of liquid-phase composition for respectively (a) catalyst spheres with data from Figure 6b. Standard operating conditions at $t = 0$ min. Liquid flow rate is changed from 6.5 ml s$^{-1}$ to respectively 10.6 ml s$^{-1}$ (o) and 2.7 ml s$^{-1}$ (Δ).and (b) structured packing elements with data from Figure 7: standard operating conditions. Open symbols: uncorrected conversion rates, closed symbols: corrected conversion rates $r_{T_s}$.

consequence of the increasing average bed temperature with flow direction through the catalyst bed: when the measured data are corrected for thermal effects they turn out to be independent of packing height.

*Liquid flow rate*

Figure 11a shows the liquid-phase composition independent conversion rates as a function of the liquid flow rate for the catalyst spheres. Both the measured conversion rates as well as the thermally corrected conversion rates are shown. Especially at low liquid flow rates, thermal effects may contribute to an increase of the conversion rate which amounts to 70% for the spheres. It can be seen that, despite correction for the thermal effects, the conversion rate increases several factors in magnitude with decreasing liquid flow rate. This phenomenon has also been observed in the literature and is believed to be due to partial wetting of the catalyst particles. For the highest flow rates (operating in the pulse flow regime) the conversion rate reaches a constant value. In Figure 11b, the fraction AMS at which the conversion rate becomes dependent on the liquid-phase composition ($x$-AMS$_{critical}$) is plotted as a function of the liquid flow rate. This critical fraction decreases with increasing liquid flow rate. At the highest liquid flow rate, corresponding to operation in the pulse flow regime, the conversion rate is independent of $x$-AMS for $x$-AMS > 0.02 which agrees with the results reported by Germain *et al.*[32], Snider and Perona[33], Funk *et al.*[34] and Cini and Harold[30]. They, however, all operated their reactor in the trickle flow regime.

Figure 12 shows the influence of the liquid flow rate on the extrapolated conversion rates (to $x$-AMS = 1) for the structured packing elements. Here also the measured conversion rates, as well as the thermally corrected conversion rates, are shown. Again at low liquid flow rates, thermal effects may contribute to a substantial increase of the conversion rate which amounts to 50% for the structured packing elements. Suprisingly, contrary to the

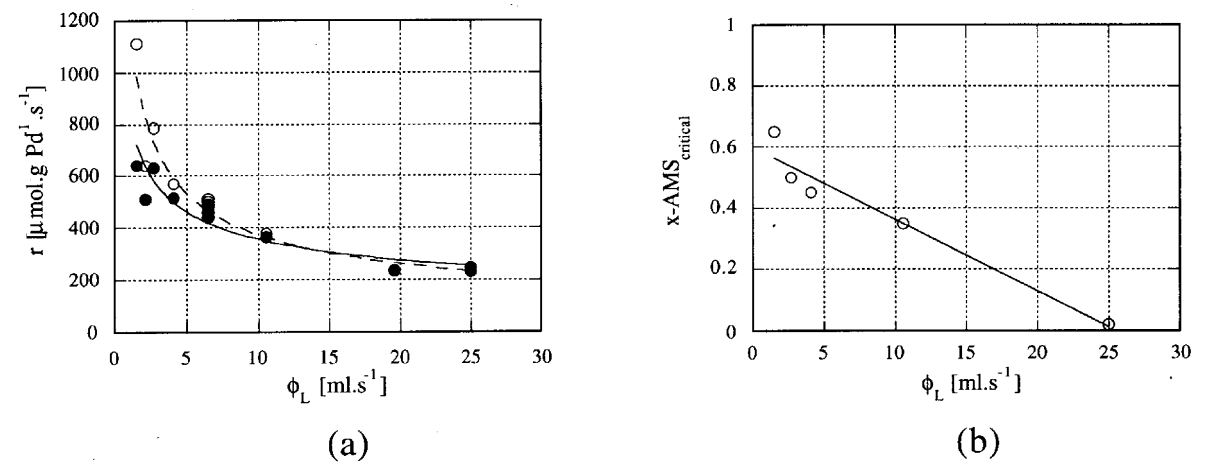


*Figure 11.* (a) Liquid-phase independent conversion rate as function of liquid flow rate. Standard operating conditions. Open symbols: uncorrected conversion rates, closed symbols: corrected conversion rates $r_{T_s}$, ( - - - ) trend line of observed conversion rates, ( —— ) trend line of corrected conversion rates. (b) Critical liquid-phase composition as function of liquid flow rate. Standard operation conditions.

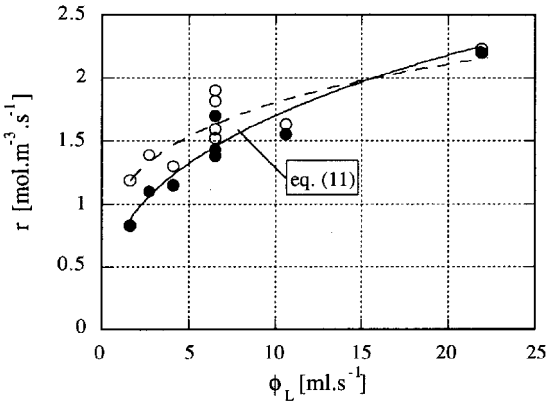


*Figure 12.* Influence of liquid flow rate on conversion rate for structured packing elements with data obtained from four separate experimental runs. (Δ), ( ) and (x) data from subsequent experiments without refilling the reactor column. Standard operating conditions. Open symbols: uncorrected conversion rates, closed symbols: corrected conversion rates $r_{T_r}$, ( - - - ) trend line of observed conversion rates, ( —— ) trend line of corrected conversion rates (equation (7)).

findings for the catalyst spheres, an increase in liquid flow rate also results in an increase of the conversion rate. For the structured packing elements, the conversion rate data, corrected for the axial temperature profile, as a function of liquid flow rate could be represented by:

$$r = 0.74\phi_L^{0.36} \tag{7}$$

## Discussion

*Spherical catalyst particles*

The activation energy of the conversion process is rather low in this case. At the highest liquid flow rate, a value of 17 kJ mole$^{-1}$ was found. This value is typical for a process which is limited by external mass transfer of hydrogen: the estimated total energy of activation, which is determined by the diffusivity of hydrogen and the solubility of hydrogen, is $13 + 4 = 17$ kJ mol$^{-1}$. At the highest liquid flow rate, the conversion rate is first order with respect to hydrogen and zero order with respect to AMS. It is therefore very likely that external hydrogen mass transfer limitation is controlling the overall conversion rate in this case.

With decreasing liquid flow rate, the conversion rate was found to increase. This effect has also been observed in the literature[31,34,35] and can be explained by partial wetting. It is thought that at the wetted part external mass transfer is the rate limiting process, whereas the hydrogen supply to the externally non-wetted part is conceived to proceed very fast and consequently the internal diffusion limited chemical reaction is rate limiting in this case.

Since the conversion rate process is partially determined by mass transfer of hydrogen and partially by internal diffusion limited chemical reaction, the activation energy of the process should vary from 17 to 29 kJ mole$^{-1}$ in case liquid flow is decreased. This agrees with the experimentally observed trend in the activation energy.

From the experiments, it could be concluded that below a certain AMS-fraction the conversion rate becomes dependent on the liquid-phase composition. The same trend has been observed by Babcock *et al.*[29] who explained the observed trend on the basis of an advanced reaction mechanism. However, they reported an activation energy of approximately 18 kJ mole$^{-1}$ which is typical for a mass transfer process. The present experimental data points can also not be represented with the reaction rate expression proposed by Turek and Lange[36]. Their kinetic expression predicts a more gradual change of the order with respect to AMS. As other authors have found zero order dependence of intrinsic reaction rate with respect to the AMS liquid-phase concentration, it is likely that diffusion limitation of AMS occurred both in the present study and in the one by Babcock *et al.*[29]. Beaudry *et al.*[37] proposed a mechanism which explains that under certain conditions the liquid-phase reactant may affect the conversion rate due to its inability to rapidly diffuse to the non-wetted catalyst areas. The liquid-phase reactant has to diffuse from the wetted surface area through the internally wetted particle to the non-wetted area. Due to the diffusion limitation of AMS, the order of the conversion rate at the non-wetted surface areas with respect to AMS will increase. The critical AMS-fraction, at which the conversion rate becomes dependent on *x*-AMS, increases with decreasing liquid flow rate. This effect can be explained by assuming that the average distance between the wetted and non-wetted areas increases with decreasing liquid flow rate. Due to diffusion limitation of AMS, the order of the conversion rate at the non-wetted surface areas with respect to AMS will increase. Consequently, the order of the conversion rate at the non-wetted surface with respect to hydrogen must decrease from 1. The decrease of the order of hydrogen has, however, not been observed experimentally as the order of the liquid-phase composition dependent part of the conversion rate curve is still first order with respect to hydrogen.

The insensitivity of the conversion rate with respect to both gas flow rate and packing height indicates respectively that operation takes place in a weak interaction regime and furthermore that the development of the radial liquid distribution is rather fast.

Since at the non-wetted areas chemical reaction is able to proceed without the possibility of fast heat removal, temperature rises may occur This may cause hot-spot formation, which has actually been observed in one experiment, where periodic temperature rises were measured ranging from 40 K to 80 K. The relatively high initial temperature rises, which were also reported by McManus *et al.*[31], are caused by preflooding of the catalyst bed. Due to preflooding, all particles contain enough liquid-phase reactant and they can take part in the reaction and cause a high initial conversion rate. After a certain time the conversion rate decreases to the steady state value.

*Structured packing elements*

The observed conversion rates for the structured packing elements in mole m$^{-3}$ s$^{-1}$, extrapolated to *x*-AMS = 1, exhibit an order of 0.36 with respect to the liquid flow rate. The specific gas-liquid contact area for chemisorption of $CO_2$ in DEA/water possesses an order of 0.4 with respect to the liquid flow rate (see equations (3) and (7)). It seems that the conversion rate and the specific gas-liquid contact area are related to each other where the wetted area provides an estimate of the packing surface area which is actually used for reaction.

The hydrogenation process exhibits first order behaviour with respect to both the fraction AMS and the fraction

hydrogen in the gas phase. The sum of both orders is therefore two. The literature shows that the chemical reaction is first order with respect to the hydrogen fraction and zero order with respect to the fraction AMS. According to the literature, the sum of the orders for the chemical reaction is therefore 1. From a theoretical point of view, the sum of both orders in the hydrogenation process should be equal to or less than the sum of the orders of the chemical reaction. That is, if the order with respect to *x*-AMS has a positive value due to mass transfer limitation of AMS, the order with respect to hydrogen should decrease from 1 by almost the same amount. So the experimentally observed findings and the theoretical expectations seem to be in contradiction and are not yet understood.

The experimentally found values for the energies of activation, ranging from 25 kJ mole$^{-1}$ at the highest liquid flow rate to 37 kJ mole$^{-1}$ at the standard liquid flow rate, are much higher than was the case for the catalyst spheres. It seems as if the hydrogenation process is governed, also to some external diffusion limitation of AMS, as well as by the intrinsic reaction rate.

As was the case for the spheres, the insensitivity of the conversion rate with respect to both gas flow rate and packing height indicates, respectively, that operation takes place in a weak interaction regime, which is in agreement with the very low observed pressure drop, and furthermore that the development of the radial liquid distribution is rather fast.

*Transport mechanisms*

For both the spheres and the structured packing, the behaviour of the experimentally determined conversion rates is not fully understood. For the spheres, the order of the conversion rate with respect to hydrogen is expected to decrease from 1 when the order of the conversion rate with respect to AMS increases due to mass transfer limitation for $x\text{-AMS} < x\text{-AMS}_{\text{critical}}$. This has, however, not been observed. For the structured packing, the sum of the orders of the conversion rate with respect to AMS and hydrogen is two. This is in contradiction with the theoretical expectations, which predict that the sum of both orders in the hydrogenation process should be equal to or less then the sum of the orders of the intrinsic chemical reaction, which is 1. A much better understanding of the results for both packing types can be obtained when it is simply assumed that the chemical reaction occurring at the catalytic surface is first order, with respect to both hydrogen and AMS.

The spheres will be completely wetted, containing well-wetted (development of pockets with stagnant liquid) and moderately-wetted areas. The wetting efficiency, defined as the fraction of the surface area which is well-wetted, increases with increasing liquid flow rate. The conversion rate at the well-wetted part of the catalyst particles will be limited by the external mass transfer of hydrogen. At the moderately wetted part, containing a thin liquid film, the conversion rate will also be limited by the external mass transfer of hydrogen, provided that the AMS-fraction, and thus the reaction rate, is sufficiently high. The conversion rate for this case will be several times faster than that for the well-wetted part. When the AMS-fraction decreases due to conversion of AMS, the chemical reaction rate will decrease and become the limiting process at the surface area covered by the thin films. The prevailing equations are able to describe the experimentally found dependences of the conversion rate on liquid flow rate and liquid-phase composition.

The structured packing will be partially wetted, containing moderately-wetted and dry areas. Now the amount of moderately-wetted surface area will increase with increasing liquid flow rate. At the moderately-wetted part, containing a very thin liquid film, the conversion rate is limited by the chemical reaction. Consequently, the conversion rate will depend on the liquid-phase composition according to $r = A + B\,x\text{-AMS}$ and secondly, high activation energies will prevail.

*Comparison of spheres and structured packing elements*

It appears that the conversion rate is mainly determined by the conversion process at the moderately-wetted surface. The largest difference between the spheres and the structured packing is the fact that for the latter packing type, the amount of moderately-wetted area can increase with increasing liquid flow rate due to the presence of dry areas, whereas for the spheres, pockets with stagnant liquid will develop with increasing liquid flow rate.

The conventional packing has well-wetted areas or stagnant liquid zones, which allows hot spots to occur. The relatively large internal reactant holdup of the spheres allows the reaction to proceed without supply of 'fresh' AMS, but consequently also without removal of reaction heat, resulting in a significant temperature rise of the stagnant liquid. In the case of the structured packing, no stagnant liquid zones are present and hence no hot spot formation is possible. Furthermore, when such a stagnant zone does occur, the temperature rise is limited, as only a small amount of reactant is present inside the catalyst. Thus, for fast exothermic liquid phase reactions, the structured packing offers better possibilities to prevent the occurrence of hot-spots. More generally, it can be said that for minimization of the chance of hot-spot formation, the holdup of the liquid-phase reactant inside the catalyst should be low. This can also be achieved by using non-porous spheres with a thin active layer at the surface. It would be very interesting to investigate whether this is true and if the results of the non-porous spheres show a closer resemblance with those of the structured packing.

Since the geometrical area of the structured packing is used more efficiently (see section giving typical results of a trickle bed experiment), it is expected that higher volumetric conversion rates are possible by using KATAPAK® elements with a larger geometrical area. Increasing the geometrical area for the spheres by using smaller particles, does not necessarily lead to increasing conversion rates as it is likely that the amount of well-wetted area (liquid pockets) will increase. Furthermore, the application of smaller particles will lead to increasing pressure drop gradients.

## CONCLUSIONS

The performances of a conventional packing consisting of small diameter spherical particles and a structured packing consisting of KATAPAK elements have been compared for a chemisorption process and a process where a heterogeneously catalysed chemical reaction is carried out. Both processes were performed in a trickle-bed reactor.

The chemisorption measurements have shown that the

specific gas-liquid contact area and the volumetric liquid-side mass transfer coefficient of the two investigated packing types are in the same order of magnitude. The structured packing has, however, a higher contact efficiency.

Both packing types show a different behaviour when the mass transfer parameters are considered as a function of the liquid flow rate. The specific gas-liquid contact area and the (volumetric) liquid-side mass transfer coefficient in the case of the structured packing, depend linearly on the liquid flow rate, whereas in the case of the dumped packing, both mass transfer parameters are not a clear function of the liquid flow rate nor show an optimum.

It is expected that higher gas-liquid contact areas and volumetric liquid-side mass transfer coefficients are possible by using a structured packing with a higher specific geometrical area. Increasing the geometrical area for the spheres by using smaller particles does not necessarily lead to increasing mass transfer parameter values. In addition, the application of smaller particles will lead to increasing pressure drop gradients. Improved mass transfer characteristics in a structured bed may also be expected at higher liquid flow rates.

The heterogeneously catalysed chemical reaction measurements have shown that the volumetric conversion rates for both packing types are also in the same order of magnitude. The structured packing has, however, a higher catalyst effectiveness.

Both packing types show a different behaviour when the conversion rate is considered as a function of liquid-phase composition. For the dumped packing, the conversion rate is independent of liquid-phase composition when the reactant fraction is sufficiently high. For the structured packing, the conversion rate always increases with increasing reactant fraction.

The most striking difference betweeen the two packing types is found when the conversion rate is considered as a function of liquid flow rate. The dumped packing shows a decreased conversion rate with increasing flow rate, whereas the structured packing shows an increased conversion rate with increasing flow rate.

The experimentally observed trends can be understood when it is assumed that the spheres are completely wetted, containing pockets with stagnant fluid, and the structured packing elements are partially wetted.

It is expected that higher volumetric conversion rates can be achieved by using a structured packing with a higher specific geometrical area as well as by applying higher liquid flow rates. Increasing the geometrical area of the spheres by using smaller particles does not necessarily lead to increasing conversion rates. In addition, the application of smaller particles will lead to increasing pressure drop gradients.

For fast exothermic liquid-phase reactions, it is better to use a structured packing since it minimizes the chance of hot-spot formation. This is due to the absence of stagnant liquid zones and its relatively low holdup of the liquid-phase reactant inside the catalyst.

## NOMENCLATURE

| | |
|---|---|
| $a_{GL}$ | specific gas-liquid contact area, $m^{-1}$ |
| $AL$ | Hinterland ratio |
| $C$ | molar concentration, $mol\,m^{-3}$ |
| $C_p$ | heat capacity, $J\,mol^{-1}K^{-1}$ |
| $D$ | diffusion coefficient, $m^2s^{-1}$ |
| $D_c$ | column diameter, m |
| $E$ | chemical enhancement factor |
| $E$ | energy of activation, $J\,mol^{-1}$ |
| $\phi$ | flow rate, $m^3s^{-1}$ |
| $G$ | gas flux, $kg\,m^{-2}s^{-1}$ |
| $h$ | packing height, m |
| $H$ | packing height, m |
| $H_t$ | total liquid holdup |
| $\Delta H_R$ | reaction heat, $kJ\,mol^{-1}$ |
| $Ha$ | Hatta number |
| $J$ | molar flux, $mol\,m^{-2}s^{-1}$ |
| $k_{app}$ | apparent first order reaction rate constant, $s^{-1}$ |
| $k$ | mass transfer coefficient, $m\,s^{-1}$ |
| $L$ | liquid flux, $kg\,m^{-2}s^{-1}$ |
| $m$ | solubility, $C_L/C_G$ |
| $n_{Pd}$ | amount of palladium, g |
| $P$ | pressure, Pa |
| $r$ | reaction or conversion rate, $mol\,g\,Pd^{-1}s^{-1}$ or $mol\,m^{-3}s^{-1}$ |
| $R$ | chemical reaction rate, $mol\,m^{-3}s^{-1}$ |
| $R$ | gas constant, $J\,mol^{-1}K^{-1}$ |
| $S$ | cross-sectional area, $m^2$ |
| $t$ | time, s |
| $T$ | temperature, K |
| $U$ | superficial velocity, $m\,s^{-1}$ |
| $x$-AMS | fraction AMS in liquid phase |
| $y$ | molar fraction in the gas phase |
| $z$ | axial coordinate, m |

*Sub- and superscripts*

| | |
|---|---|
| *adiab* | adiabatic |
| *AMS* | α-methylstyrene |
| *app* | apparent |
| *exp* | experimental |
| *G* | gas phase |
| *L* | liquid phase |
| *sep* | gas-liquid separator |
| *t* | total |

## REFERENCES


1. Schuit, G. C. A. and Gates, B. C., 1973, Chemistry and engineering of catalytic hydrodesulphurization, *AIChEJ*, 19: 417–438.
2. Satterfield, C. N., 1975, Trickle-bed reactors, *AIChEJ*, 21: 209–228.
3. Morsi, B. I., Laurent, A., Midoux, N., Barthole-Delaunay, G., Storck, A. and Charpentier, J. C., 1984, Hydrodynamics and gas-liquid-solid interfacial parameters of co-current downward two-phase flow in trickle-bed reactors, *Chem Eng Commun*, 25: 267–293.
4. Ramachandran, P. A., Dudukovic, M., P. and Mills, P. A., 1987, Recent advances in the analysis and design of trickle-bed reactors, *Sadhana* 10: 269–298.
5. Meier, W., Stoecker, W., D. and Weinstein, B., 1977, Performance of a new, high efficiency packing, *Chem Eng Prog*, 73(11): 71–77.
6. DeGarmo, J. L., Parulekar, V., N. and Pinjala, V., 1992, Consider reactive distillation, *Chem Eng Prog*, 88(3): 43–50.
7. Laso, M., Henriques de Brito, M., Bomio, P. and von Stockar, U., 1995, Liquid-side mass transfer characteristics of a structured packing, *Chem Eng J*, 58: 251–258.
8. Johannisbauer, W. and Jeromin, L., 1992, Structured column packings in the oleochemical industry, *IChemE Symp Series* No 128: B77–B83.
9. Krafczyk, J. and Gmehling, J., 1994, Einsatz von Katalysatorpackungen für die Herstellung von Methylacetat durch reaktive Rektifation, *Chem Ing Tech*, 66: 1372–1375.
10. Reiss, L. P., 1967, Cocurrent gas-liquid contacting in packed columns. *Ind Eng Chem Proc Des Dev*, 6: 486–499.
11. Gianetto, A., Baldi, G. and Specchia, V., 1970, Absorption in packed towers with cocurrent downward high-velocity flows - part I: interfacial areas, *Quad Ing Chim Ital*, 6: 125–133.
12. Gianetto, A., Specchia, V. and Baldi, G., 1973, Absorption in packed towers with concurrent downward high-velocity flow - part II: mass transfer, *AIChEJ*, 19: 916–922.
13. Goto, S. and Smith, J. M., 1975, Trickle-bed reactor performance - part I: holdup and mass transfer effects, *AIChEJ*, 21, 706–713.

14. Charpentier, J. C., 1976, Recent progress in two phase gas-liquid mass transfer in packed beds, *Chem Eng J*, 11: 161–181.
15. Fukushima, S. and Kusaka, K., 1977, Interfacial area and boundary of hydrodynamic flow region in packed column with cocurrent downward flow, *J.Chem Eng Jap*, 10: 461–467.
16. Fukushima, S. and Kusaka, K., 1977, Liquid-phase volumetric and mass-transfer coefficient, and boundary of hydrodynamic flow region in packed column with cocurrent downward flow, *J Chem Eng Jap*, 10: 468–474.
17. Mahajani, V., V. and Sharma, M. M., 1979, Effective interfacial area and liquid side mass transfer coefficient in trickle bed reactors, *Chem Eng Sci*, 34: 1425–1428.
18. Morsi, B., I. and Charpentier, J. C., 1983, Hydrodynamics and gas-liquid interfacial parameters with organic and aqueous liquids in catalytic and non catalytic packings in trickle-bed reactors, *NATO ASI Ser*, Ser. E, 73(2): 133–159.
19. Midoux, N., Morsi, B. I., Purwasasmita, M., Laurent, A. and Charpentier, J. C., 1984, Interfacial area and liquid side mass transfer coefficient in trickle bed reactors operating with organic liquids, *Chem Eng Sci*, 39: 781–794.
20. Morsi, B. I., 1989, Mass transfer coefficients in a trickle-bed reactor with high and low viscosity organic solutions, *Chem Eng J*, 41: 41–48.
21. Lara-Marquez, A., Menguy, Y. and Wild, G., 1991, Determination des parametres de transfert de matiere gas-liquide dans un reacteur a lit fixe a cocourant ascendant de gaz et liquide. In *Récents Progrès en Génie des Procédés* 16: 135–140.
22. Wild, G., Larachi, F. and Charpentier, J. C., 1992, Heat and mass transfer in gas-liquid-solid fixed bed reactors, In *Heat and Mass Transfer in Porous Media*, (Elsevier, Amsterdam), 615–632.
23. Bravo, J. L., Rocha, J., A. and Fair, J. R., 1992, A comprehensive model for the performance of columns containing structured packings. *IChemE Symp Series* No 128: A489–A507.
24. Henriques de Brito, M., von Stockar, U. and Bomio, P., 1992, Predicting the liquid phase mass transfer coefficient - kL - for the Sulzer structured packing Mellapak, *IChemE Symp Series*, No 128: B137–B144.
25. Weiland, R. H., Ahlgren, K., R. and Evans, M., 1993, Mass-transfer characteristics of some structured packings, *Ind Eng Chem Res*, 32: 1411–1418.
26. Henriques de Brito, M., von Stockar, U., Menendez Bangerter, A., Bomio, P. and Laso, M., 1994, Effective mass-transfer area in a pilot plant column equipped with structured packings and with ceramic rings, *Ind Eng Chem Res*, 33: 647–656.
27. Frank, M. J. W., 1996, Mass and heat transfer phenomena in G-L(-S) reactors relevant for reactive distillation, *PhD Thesis*, (Twente University, Enschede, The Netherlands).
28. Shi and Mersmann, 1985,
29. Babcock, B. D., Mejdell, G., T. and Hougen, O. A., 1957, Catalysed gas-liquid reactions in trickling-bed reactors, *AIChEJ*, 3: 366–372.
30. Cini, P. and Harold, M. P., 1991, Experimental study of the tubular multiphase catalyst, *AIChEJ*, 37: 997–1008.
31. McManus, R. L., Funk, G. A., Harold, M., P. and Ng, K. M., 1993, Experimental study of reaction in trickle-bed reactors with liquid maldistribution, *Ind Eng Chem Res*, 32: 570–574.
32. Germain, A. H., Lefebvre, A. G. and L'Homme, G. A., 1974, Experimental study of a catalytic trickle bed reactor, *ACS*, 133: 164–180.
33. Snider, J., W. and Perona, J. J., 1974, Mass transfer in a fixed-bed gas-liquid catalytic reactor with concurrent upflow, *AIChEJ*, 20: 1172–1177.
34. Funk, G. A., Harold, M., P. and Ng, K. M., 1991, Experimental study of reaction in a partially wetted catalytic pellet, *AIChEJ*, 37: 202–214.
35. Herskowitz, M., Carbonell, R., G. and Smith, J. M., 1979, Effectiveness factors and mass transfer in trickle-bed reactors, *AIChEJ*, 25: 272–283.
36. Turek, F. and Lange, R., 1981, Mass transfer in trickle-bed reactors at low Reynolds number, *Chem Eng Sci*, 36: 569–579.
37. Beaudry, E. G., Dudukovic, M., P. and Mills, P. L., 1987, Trickle-bed reactors: liquid diffusional effects in a gas-limited reaction, *AIChEJ*, 33: 1435–1447.
38. Versteeg, G., F. and Oyevaar, M. H., 1989, The reaction between $CO_2$ and diethanolamine at 298 K, *Chem Eng Sci*, 44: 587–591.
39. Littel, R. J., 1991, Selective carbonyl sulfide removal in acid gas treating processes, *PhD Thesis*, (Twente University, Enschede, The Netherlands).
40. Versteeg, G. F., 1986, Mass transfer and chemical reaction kinetics in acid gas treating processes, *PhD Thesis*, (Twente University, Enschede, The Netherlands).
41. Snijder, E. D., 1992, Metal hydrides as catalysts and hydrogen suppliers, *PhD Thesis*, (Twente University, Enschede, The Netherlands).
42. Westerterp, K. R., van Swaaij W. P. M. and Beenackers A. A. C. M., 1990, *Chemical Reactor Design and Operation*, (Wiley & Sons, UK).

## ACKNOWLEDGEMENTS

These investigations were supported by the Foundation for Chemical Research in the Netherlands (S.O.N.). The authors also acknowledge W. Leppink for his technical support and G. Nijhuis, F. Borre, M. Scheepers and R. Röeling for their contribution to the experimental work. They are further indebted to the Sulzer company, who kindly provided the KATAPAK®-MK elements, and to the Engelhard company, who provided the catalyst spheres and carried out the Pd-impregnation of the KATAPAK®-MK elements.

## ADDRESS

Correspondence concerning this paper should be addressed to Dr J. A. M. Kuipers, Department of Chemical Engineering, Twente University, PO Box 217, 7500 AE, Enschede, The Netherlands (E-mail: J.A.M.Kuipers@ct.utwente.nl).

*The manuscript was received 26 October 1998 and accepted for publication after revision 24 May 1999.*